

# Structural investigations on yttria - doped zirconia nanopowders obtained by sol-gel method

B. S. VASILE, C. GHITULICA, N. POPESCU-POGRION<sup>a,\*</sup>, S. CONSTANTINESCU<sup>a</sup>, I. MERCIONIU<sup>a</sup>, R. STAN, E. ANDRONESCU

University POLITEHNICA from Bucharest, Faculty of Applied Chemistry and Materials Science, 1-7, Polizu street, sect. 1, 011061, Romania

<sup>a</sup>National Institute of Materials Physics, 105 bis Atomistilor Street, Bucharest-Magurele, P.O. Box MG-7, code 077125, Romania

The attractive properties of zirconia, particularly fracture toughness, wear resistance and chemical stability, have led to vast research efforts designed to investigate, characterize and develop such materials. Applications vary from structural, mechanical, biomedical to electrical, especially the fuel cells field. The current study is aiming at preparation and structural characterization of 10% Y<sub>2</sub>O<sub>3</sub> stabilized ZrO<sub>2</sub> nanometric powders. The sol-gel method is known to be easy to use for producing various kinds of materials, structured at nanometric level, so was chosen for the elaboration of powders. Different thermal treatments were applied to the obtained materials, which were consequently investigated through thermal analysis, X-ray diffraction (XRD) scanning electron microscopy (SEM) and transmission electron microscopy (TEM). The characteristics of Y<sub>2</sub>O<sub>3</sub> doped zirconia powders are influenced by the processing parameters and proved promising for further applications in, for example, the Solid Oxides Fuel Cell field.

(Received November 30, 2007; accepted December 5, 2007)

*Keywords:* ZrO<sub>2</sub>, nanopowder, Sol-gel method, XRD, TEM

## 1. Introduction

The main problem of IT-SOFC's is the severe requirements that the electrolytes used have to satisfy, which among others are the following: (a) phase stability in both reducing and oxidising atmospheres for long periods of time in service ( $\geq 5000$  h); (b) high and stable electrical conductivity ( $\geq 10^{-2}$  S·cm<sup>-1</sup>) at the fuel cell operating temperature; and (c) relatively high mechanical properties ( $\sigma \geq 500$  Mpa at room temperature and  $K_{IC} \geq 3$  Mpa m<sup>1/2</sup>).

Zirconia ceramics containing 3 mol % of Y<sub>2</sub>O<sub>3</sub> and having a tetragonal structure, (Y-TZP) are currently being used, because of their strength and fracture toughness. However, at present there are two main problems with this kind of electrolyte: its low ionic conductivity at the SOFC operating temperature and, on the other hand, its very bad ageing behaviour, given the metastability of the tetragonal zirconia solid solutions.

Although zirconia ceramics containing between 3 and 6.5 mol% Y<sub>2</sub>O<sub>3</sub> (Y-PSZ) presented better ageing behaviour and higher ionic conductivity, these properties could be seriously affected by the characteristics and annealing behaviour of a dual (tetragonal + cubic) microstructure, typical for these kinds of zirconia ceramics.

Fully stabilised zirconia (FSZ), with a cubic structure, containing 6.5 and 10 mol % Y<sub>2</sub>O<sub>3</sub>, is the most attractive zirconia ceramic to be used as an electrolyte in SOFC systems, due to its improved electrical properties. However, it must be noted that both the mechanical and thermal properties of these zirconia ceramics are not as good as desired and consequently many efforts are being

made to optimise them. The preparation of nanostructured materials could be an important step forward in that direction [1,2].

## 2. Experimental

### 2.1. Sol-gel preparation

The method chosen for the preparation of yttria-stabilized zirconia is the sol-gel process. The sol-gel process consists in preparing a sol, jellying the sol and then removing the solvent, followed by an appropriate thermal treatment. The sol can be obtained from organic or inorganic precursors (alcoxides, silica-gel, nitrates, etc.) and it consists of dense particles of oxides or polymeric clusters (clusters of polymeric chains) fine dispersed in the liquid phase.

The precursors used for preparation of yttria (10mol%) stabilized zirconia were zirconium propoxid (FLUKA – Zirconium (IV) Propoxid Solution 70% in Propanol) and yttrium butoxid (ALDRICH – Yttrium (II) butoxid, 0,5M Solution in Toluene, 99,9%). Both alcoxides are showing a large hydrolysis reaction velocity, that makes them not suitable for sol-gel processes. In order to obtain alcoxides with higher stability, 2-metoxiethanol was added to both precursor solutions, until a concentration of 0.25M was reached.

The precursors were mixed into a molar ratio Y<sub>2</sub>O<sub>3</sub>/ZrO<sub>2</sub> of 1/10. The hydrolysis agent – water is also mixed with 2-metoxiethanol, in a concentration of 0.25M. Once the water was added, the mixture started jellying

quickly, the process being completed in an interval of approximately 20 minutes.

The obtained gel is left to mature for 2.5 hours and then dried for 36 hours into a stove, at the temperature of 110°C. The powder obtained is grounded and thermally treated at temperatures between 500 – 1000°C, with a soaking time of 2 hours and with a speed of temperature growth of 10°C/minute [3,4].

## 2.2. Characterization of the nano-powders

The obtained powder was characterized using thermal analysis, laser granulometry, scanning electron microscopy, X-ray diffraction (DRX) and transmission electron microscopy (TEM) with selected area electron diffraction (SAED).

### 2.2.1. Thermal analysis experimental aspects

The Y<sub>2</sub>O<sub>3</sub> (10 mol %) doped ZrO<sub>2</sub> nano-powders, obtained through the sol – gel method (YSZ) were investigated through thermal analysis. The thermal differential analysis and thermogravimetry diagrams were obtained using a DTA-50 SHIMADZU equipment, in normal conditions of temperature and pressure (T=300k, P=1 atm). The powder was put into a platinum nacelle and heated up to 1000 °C, with a temperature growing rate of 10°C/minute.

### 2.2.2. XRD experimental aspects

The Y<sub>2</sub>O<sub>3</sub> (10 mol %) doped ZrO<sub>2</sub> powders, obtained through sol – gel method (YSZ) were investigated through XRD. The spectra have been obtained by the DRON\_2 equipment (2θ/min=0.500), intensity 1000 counts/s, 2 x 0.044 step/s) in normal conditions of temperature and pressure (T=300K, P=1 atm), using the K<sub>α</sub>-Cu X-ray of λ=1.54056Å. Calibration of the 2θ scale was obtained with the XRD lines of In<sub>2</sub>O<sub>3</sub> (a= 10.117Å, spatial group Ia3). The spectra have been fitted by specialized soft taking into account Lorentz or Gauss shape of the XRD lines. The errors of the intensity, XRD line position and of its half - linewidth (linewidth at half intensity) are ±2.5 and respectively ± 0.045°.

### 2.2.3. Electron microscopy experimental aspects

An JEOL- 200CX Scanning Transmission Electron Microscope, with the following characteristics: resolution - 0.45 nm lattice image attainable, accelerating voltage - 40 kV SEM / 200 kV TEM, magnification range 100X-330kX, full range of sample holders, including heating, cooling and double tilt analytical, was used in investigations.

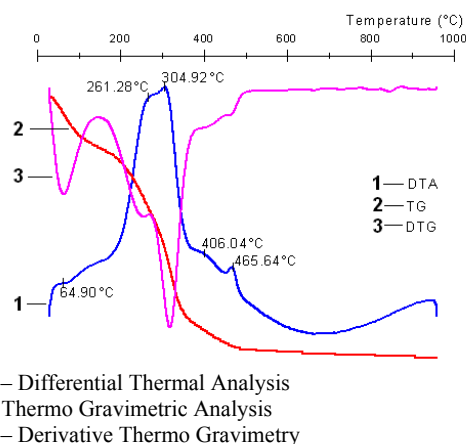
The YSZ (10 mol% Y<sub>2</sub>O<sub>3</sub>) nano-powders were applied on glass microscope lamella with 2% colloid in amyl acetate. The films were removed from the lamella substrates by immersion in distilled water; floated off on the electron microscope copper grids and were fixed with carbon thin films deposited in vacuum in a deposition

installation type JEOL [5]. For scanning investigations the powder was put on the microscope lamella (15 x 3) mm covered with Al thin films, and put on the special holder for SEM investigations [5].

## 3. Results and discussions

### 3.1. Thermal analysis results

In Fig. 1 is plotted the thermal analysis diagram of the YSZ (10mol% Y<sub>2</sub>O<sub>3</sub>) powder, obtained through the sol-gel method.



DTA – Differential Thermal Analysis  
TG – Thermo Gravimetric Analysis  
DTG – Derivative Thermo Gravimetry

Fig. 1. Thermal analysis diagram of YSZ (10mol% Y<sub>2</sub>O<sub>3</sub>) raw nano-powders obtained through the sol-gel method.

The total mass loss is of 26.196%. The effects are due to the evaporation of water (~60 °C), the decomposition of organic substances (~ 250 – 310 °C), respectively to the combustion of residual carbon (~470 °C) [1].

### 3.2 XRD results

In the Fig. 2, the XRD spectra of synthesized and calcinated (1000 °C 2h) samples were plotted.

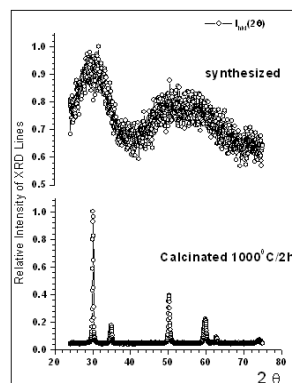


Fig. 2. The XRD spectra of calcinated -1000 °C for 2h (bottom spectra) and synthesized (upper spectra) for sol-gel samples  $\theta$ .

The figure reveals the effect of the thermal treatment (at 1000 °C) on sol-gel samples. In the case of the synthesized samples, the XRD spectra have very broad and unresolved lines.

The fit of the sample treated at 1000 °C for 2 hours is shown in Fig. 4. It presents narrow lines ( $\Gamma_{2\theta} = [0.12 \pm 0.30^\circ]$ ), which are denoting a high crystallization. The fit procedure was applied using the Gaussian and Lorentzian multi-peak functions. In the case of a single phase and a high crystallization, the spectrum is a sum of Lorentzian peaks. The presence of several phases complicates the spectra, as a consequence of the superposition of two or more XRD contributing peaks of different phases. As one can observe in Fig. 4, the convergence parameter  $r^2$  shows good fits both for the Lorentzian and Gaussian multi-peak functions, but the best fit of the spectrum is obtained for the last one. That suggests the presence of at least two contributions corresponding to different phases.

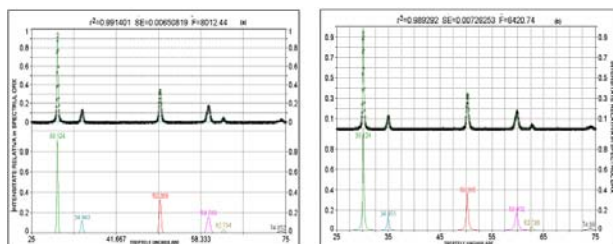


Fig. 3. The best fit of the  $Y_2O_3$  (10 mol %) doped  $ZrO_2$  sol-gel – calcinated at 1000°C/2h – spectra (left hand - Gaussian and right hand - Lorentzian multi-peaks fit), where  $r^2$  is the convergence parameter of the fit.

Indeed, the best fit of the most intense XRD line of spectrum reveals the presence of two Lorentzian peaks with relative areas  $70 \pm 5\%$  and  $30 \pm 5\%$  at  $2\theta = 30.003 \pm 0.090^\circ$  and respectively  $30.119 \pm 0.090^\circ$  (see Fig. 3).

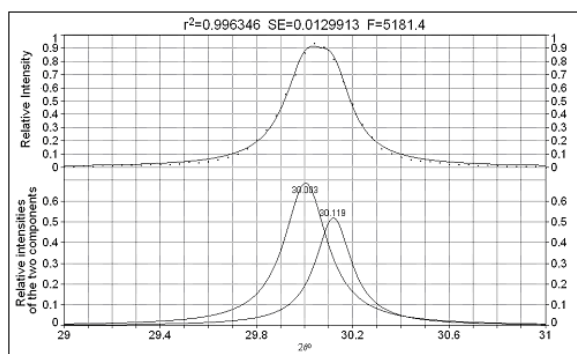


Fig. 4. The refined fit of the most intense XRD-line for sol-gel  $Y_2O_3$  (10 mol %) doped  $ZrO_2$  – calcinated at 1000 °C for 2 hours.

Those correspond to the cubic (FM3M symmetry group) phase with  $a=5.1542\text{\AA}$  and tetragonal ( $P4_2/nmc$ )

one, with  $a=b=3.619\text{\AA}$ ,  $c=5.17\text{\AA}$ , taking into account the Bragg-relation  $2d_{h,k,l}\sin\theta = n\lambda$ .

The reported values of the cubic and tetragonal phases are  $a = 5.1473\text{\AA}$ ,  $5.1482\text{\AA}$ ,  $5.1600\text{\AA}$ , and  $5.2100\text{\AA}$  (in [75316], [60610], [60605], [60396] and [60400] ASTM files) and respectively  $a=b=3.5925\text{\AA}$ ,  $3.6067\text{\AA}$ ,  $c=5.1837\text{\AA}$ ,  $5.129\text{\AA}$  (in [68781], [70014] and [709015] ASTM files). The similarity of our XRD spectra, with the reported ones for YSZ cubic and tetragonal phases, confirms the presence of the YSZ in two crystalline phases with a preponderant cubic phase ( $\sim 7/3$ ). The difference in the unit-cell parameter  $a$ , might be given by an oxygen deficiency in the cubic structure.

The XRD spectra of the sol-gel samples, thermally treated at different temperatures, reveal the narrowing process of the diffraction lines (see Fig. 6a), suggesting the growth of  $Y_2O_3$  (10 mol %) doped  $ZrO_2$  crystallites.

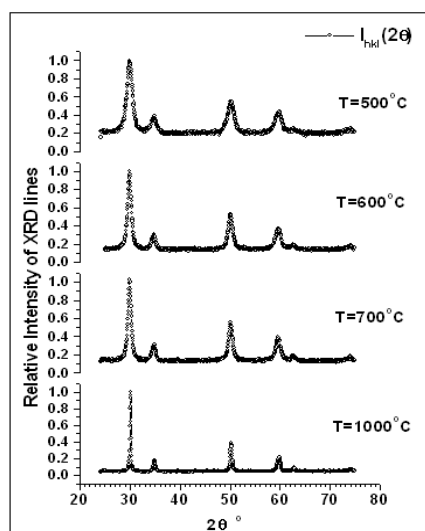


Fig. 5a. The XRD spectra of the  $Y_2O_3$  (10 mol %) doped  $ZrO_2$  prepared by sol-gel method, calcinated at different temperatures (500, 600, 700, 1000°C for 2 hours).

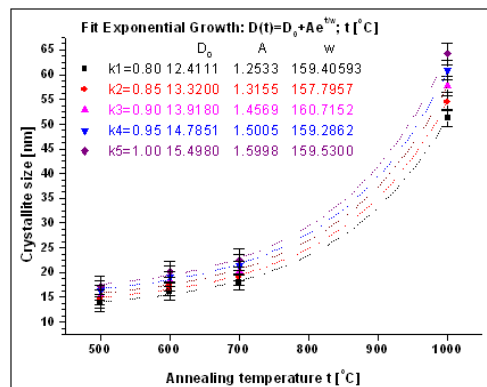


Fig. 5b. The exponential growth fit of particle size for the heat-treated sol-gel  $Y_2O_3$  (10 mol %) doped  $ZrO_2$  sample, using Debye - Scherrer equation for different values of  $K$ .

The average crystallite size of all heat-treated samples has evaluated from the line broadening of the (220) peak using the Scherrer equation [8 -10]:

$$D_m = \frac{K \cdot \lambda}{\beta_{1/2} \cdot \cos\theta}$$

Where  $D_m$  is the average crystallite size in [Å],  $K$  is a constant depending of the morphology of the investigated samples. The constant  $K$  is typically close to unit and ranges from 0.8÷1.39.  $\lambda$  is the wavelength of the incident x-ray and  $\theta$  is the corresponding Bragg angle.

Here  $\beta_{1/2} = \sqrt{(\beta_{1/2})_o^2 - b_o^2}$  where  $(\beta_{1/2})_o$  is the full width at half maximum (FWHM) of the (220) peak [rad].  $\lambda$  has considered 1.54056 Å and  $b_o$  is FWHM of (220) peak from XRD spectrum of control YSZ sample, heat-treated at 1000°C for 2h,  $b_o = 0.13$  [grd], corresponding to 0.002269 [rad]. The exponential growth fit of crystallites have plotted for different values of  $K$  in Figure 5b. The best agreement of estimated  $D_m$  with the average crystallites size observed by TEM is given for  $K = 0.80 \div 0.90$ . That is corresponding to the observed morphology on the investigated samples by electron microscopy techniques (see Table 1).

Table 1. The average particle size of YSZ obtained by the sol-gel procedure and calcined at 500-1000°C, using the Scherrer equation, and significant values of  $K$ .

Sample Y <sub>2</sub> O <sub>3</sub> (10 mol %) doped ZrO <sub>2</sub>	Calcination temperature [°C]	$(\beta_{1/2})_o$ [grd]	$\theta$ [grd]	Medium grain size		
				K=0.80	K=0.90	K=1.00
				[10 <sup>-9</sup> m]	[10 <sup>-9</sup> m]	[10 <sup>-9</sup> m]
Sol-gel	500	0.58	25.13	13.8	15.5	17.2
	600	0.50	25.06	16.1	18.2	20.2
	700	0.45	25.07	18.1	20.4	22.6
	1000	0.20	25.13	51.3	57.7	64.2
Average Errors		±0.05	±0.06	±1.72	±1.94	±2.15

### 3.3. SEM results

The micrograph obtained on 10% yttria doped zirconia nanopowder calcinated at 1000°C/2h is presented in Fig. 8.

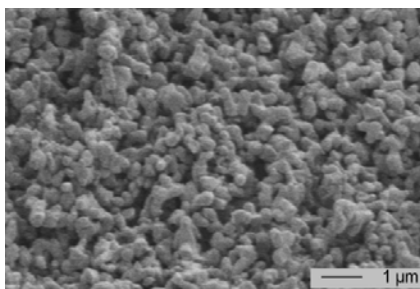


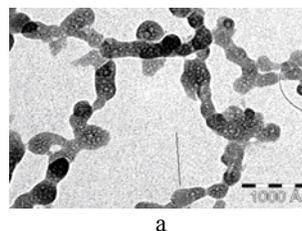
Fig. 6. Scanning electron microscopy image on Y<sub>2</sub>O<sub>3</sub> (10 mol %) doped ZrO<sub>2</sub> synthesized nano-powders obtained by sol-gel.

From SEM image obtained on 10% yttria doped zirconia nano-powder calcinated at 1000°C we can observe a high tendency to form agglomerates, with a maximum size of 1 μm. Granules as small as 0.1 μm can also be visualized.

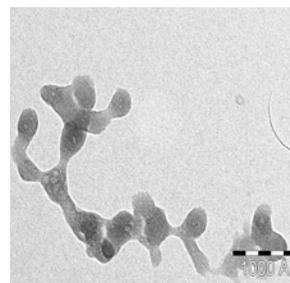
### 3.4. TEM results

In Figs. 7 – 10 are presented transmission electron microscope micrographs, in correlation with selected area diffraction patterns, for Y<sub>2</sub>O<sub>3</sub> (10 mol %) doped ZrO<sub>2</sub> sol – gel nano-powders, synthesized and calcinated at 500, 600, 700 and 1000°C for 2 hours. Statistical methods were used

to calculate the mean diameter of particles, the repartitions and errors, measurements were made on approximately 1000 particles.



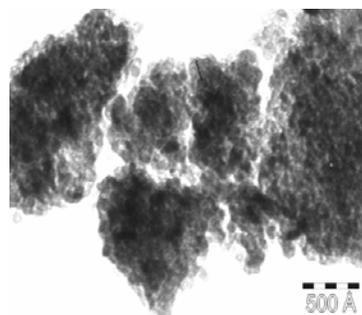
a



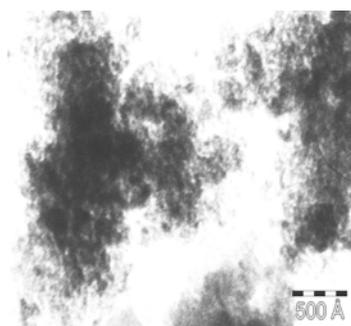
b

Fig. 7 (a, b). Transmission electron microscopy images on Y<sub>2</sub>O<sub>3</sub> (10 mol %) doped ZrO<sub>2</sub> noncalcinated nano-powders obtained by sol-gel.

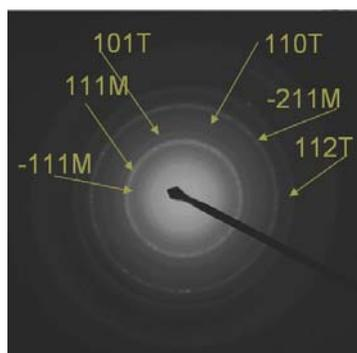
Analyzing the transmission electron microscopy images one observes the presence of spherical, uniform and porous particles, with a mean diameter of  $d_{MPO} = 32 \pm 0.828$  nm.



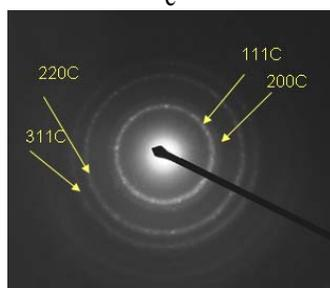
a



b



c



d

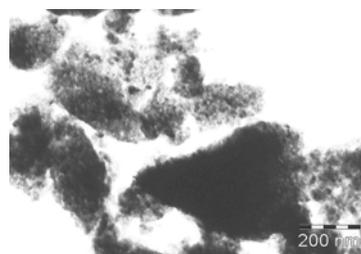
**Fig. 8.** Transmission electron microscopy images (a, b) and selected area electron diffraction patterns (c, d) on  $Y_2O_3$  (10 mol %) doped  $ZrO_2$  nano-powders calcinated at  $500^\circ C$  for 2 hours.

For the  $Y_2O_3$  (10 mol %) doped  $ZrO_2$  sol-gel nano-powders (figure 8), calcinated at  $500^\circ C$ , one observes particles with a spherical shape, with the mean diameter  $d_{Mp500} = 14.18 \pm 0.982$  nm, which tend to form agglomerates with  $d_{Ma500} = 111 \pm 1.242$  nm. From selected

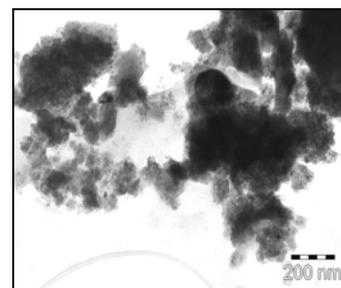
area electron diffraction patterns one observes - the presence, in different points of the Cu grid, of the following crystallographic phases: monoclinic [ASTM 83-0940], tetragonal [ASTM 81-1547] and cubic [ASTM 81-1551]; with the cubic phase as predominant (58%). The percentage of each phase is determinate by indexing, on around 25 patterns, in different points of the grids (selected maps).

The same evolution one observes for a calcination temperature of  $600^\circ C$ , but with 84% cubic phase.

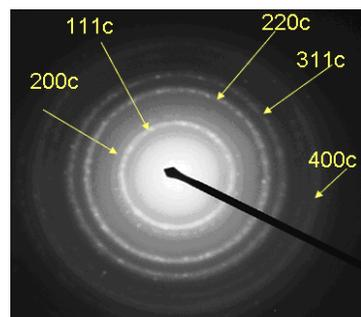
A growth of the particles and agglomerates sizes was observed also for a calcinations temperature of  $700^\circ C$  (figure 9). The selected area electron diffraction patterns have revealed only the cubic polymorph of zirconia (ASTM 81-1551).



a



b

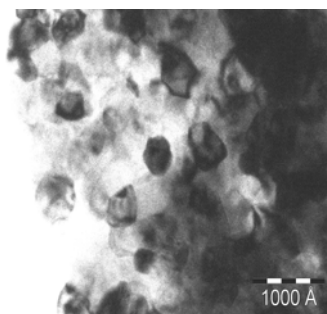


c

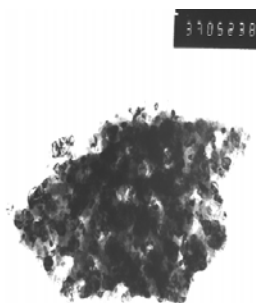
**Fig. 9.** Transmission electron microscopy images (a, b) and selected area electron diffraction pattern (c) on  $Y_2O_3$  (10 mol %) doped  $ZrO_2$  nano-powders calcinated at  $700^\circ C$ .

For the sol-gel  $Y_2O_3$  (10 mol %) doped  $ZrO_2$  powders, calcinated at the  $1000^\circ C$ , the selected area electron diffraction patterns show the cubic solid solution (ASTM 81-1551), as the predominant phase (Fig. 12c). The

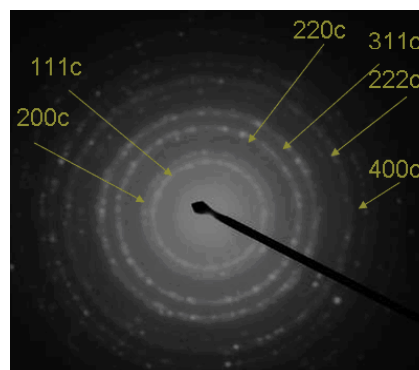
dimensions of the particles increase up to  $d_{M_p1000} = 42.85 \pm 0.884$  nm (Fig. 10a, b).



a



b



c

Fig. 10. Transmission electron microscopy images (a, b) and selected area electron diffraction patterns (c) on  $Y_2O_3$  (10 mol %) doped  $ZrO_2$  nano-powders calcinated at  $1000^\circ C$ .

The summary of the electron microscopy results are shown in the Table 2.

Table 2 The morphology of the investigated YSZ samples by electron microscopy techniques.

Sample $Y_2O_3$ (10 mol %) doped $ZrO_2$	Calcined temperature [ $^\circ C$ ]	Size value /agglomerate [nm]	Average size value /agglomerate [nm]	Size value /crystallites [nm]	Average size value /crystallites [nm]	Morphological characterization
Sol-gel	noncalcinated	-	-	18.5÷74.4	32±0.828	The particles are spherical and homogenous with a porosity $p \cong 5.2\%$ .
	500	40.5÷150	111±1.242	7.5÷18.4	14.18±0.982	The initial crystallites are spherical; agglomerates are also spherical; spherical agglomerates $\cong 42\%$ .
	600	70.5÷200.15	111±1.848	8.2÷20.5	16.85±0.822	The initial crystallites are spherical; agglomerates are also spherical; spherical agglomerates proportion $\cong 58\%$ .
	700	150÷350	150±5.242	10.2÷40	20.42±0.872	The initial crystallites are spherical; agglomerates are also spherical; spherical agglomerates proportion $\cong 65\%$ .
	1000	-	-	24.42÷75.45	42.85±0.884	In this sample are 2 particles type: - •spherical, homogenous particles; •polyhedral particles with round edges approximated by spherical

#### 4. Conclusions

Fully stabilized zirconia powders were obtained through the sol-gel method, starting from zirconium propoxid and yttrium butoxid as precursors. The samples

were calcinated at temperatures between 500 and  $1000^\circ C$  and analysed through thermal analysis, SEM, XRD, TEM and selected area electron diffraction SAED.

The temperature evolution of XRD-spectrum for the sol-gel  $Y_2O_3$  (10 mol %) doped  $ZrO_2$  samples reveals the

narrowing process of the diffraction lines, suggesting the growth of  $Y_2O_3$  (10 mol %) doped  $ZrO_2$  crystallites. The temperature dependence of the X-ray diffraction line width corresponding to the plane [220] permits to estimate the temperature dependence of the average grain-size. That varied between 15 and 70 nm, for different calcinations conditions.

The fit of the most intense XRD-line of the sol-gel and commercial  $Y_2O_3$  (10 mol %) doped  $ZrO_2$  – calcinated at  $1000^\circ C$  spectra, allowed the identification of tetragonal phase, in addition to cubic zirconia, which is predominant.

The microstructural analyses have shown the presence of nanometric powders, generally spherical, with high porosity for the synthesized samples. Agglomerates were present in the calcinated samples. An increase of grain and agglomerates sizes with higher temperature was observed. Samples treated at intermediary temperatures revealed the presence of monoclinic, tetragonal and cubic polymorphs of zirconia [7]. Starting with  $700^\circ C$ , the only phase identified through SAED was the cubic solid solution.

The 10% yttria-stabilized zirconia powders prepared by sol-gel methods are showing promising characteristics for application in the IT-SOFC electrolyte.

#### Acknowledgements

The authors express the gratitude for financial support to MEC/PNCDI/CEEX.

#### References

- [1] K. S. Mazdiyasi, Gel technology in ceramics, High Tech. Ceramics, edited by P. Vicenzini, Elsevier Science Publishers B.V., Amsterdam, 693, 1987.
- [2] J. D. Wright, N. A. J. M. Sommerdijk, Sol-gel Materials Chemistry and Applications, Gordon and Breach Science Publishers, 2001.
- [3] A. J. Lecloux, S. Nonet, F. Noville, J. P. Pirard, *Annales de Chimie, Science des Materiaux*, **16**, 77-90, (1991).
- [4] G. Antonioli, P. P. Lottici, I. Manzini, G. Gnappi, A. Montenero, F. Paloschi, P. Parent, *J. Non-Cryst.Solids* **177**, 179-186 (1994).
- [5] N. Popescu-Pogrion, R. Bercia, M. Tirnovan, *J. Optoelectron. Adv. Mater.* **6**(3), 1071 – 1076 (2004).
- [6] R. Moreno, *Am. Ceram. Soc. Bull.* **71** (10)(1972) 1521 (ME).
- [7] Vannon, R. M., Rhodes W. H., Heuer, A. H. J. *Am. Ceram. Soc.* **63** 46, (1980) (ME).
- [8] H. P. Klug, L.A. Alexander-ray Diffraction Procedures for Polycrystalline and Amorphous Materials, ed. Wiley, New-York, 1966, 491.
- [9] Y-H, Lee, Ch-W, Kuo, I-M, Hung, K-Z, Fung, M-Ch, Wang, *Journal of Non-Crystalline Solids* **351**, 3709 (2005).
- [10] Z. Zhao, L. Zhang, Y. Song, W. Wang, J. Wu, *Scripta Materialia.* **55**, 819 (2006).

\*Corresponding author: pogrion@infim.ro